

Predictions for high energy neutrino cross-sections from the ZEUS global PDF fits

Amanda Cooper-Sarkar

Particle Physics, University of Oxford, Keble Road, Oxford OX1 3RQ, UK

Subir Sarkar

*Rudolf Peierls Centre for Theoretical Physics, University of Oxford,
1 Keble Road, Oxford OX1 3NP, UK*

(Dated: February 9, 2022)

We have updated predictions for high energy neutrino and antineutrino charged current cross-sections within the conventional DGLAP formalism of NLO QCD using a modern PDF fit to HERA data, which also accounts in a systematic way for PDF uncertainties deriving from both model uncertainties and from the experimental uncertainties of the input data sets. Furthermore the PDFs are determined using an improved treatment of heavy quark thresholds. A measurement of the neutrino cross-section much below these predictions would signal the need for extension of the conventional formalism as in BFKL resummation, or even gluon recombination effects as in the colour glass condensate model.

I. INTRODUCTION

Predictions of neutrino cross-sections at high energies have sizeable uncertainties which derive largely from the measurement uncertainties on the parton distribution functions (PDFs) of the nucleon. In the framework of the quark-parton model, high energy scattering accesses very large values of Q^2 , the invariant mass of the exchanged vector boson, and very small values of Bjorken x , the fraction of the momentum of the incoming nucleon taken by the struck quark. Thus when evaluating uncertainties on high energy neutrino cross-sections it is important to use the most up to date information from the experiments at HERA, which have accessed the lowest- x and highest Q^2 scales to date. The present paper uses the formalism of the ZEUS-S global PDF fits [1], updated to include *all* the HERA-I data.

Conventional PDF fits use the Next-to-leading-order (NLO) Dokshitzer-Gribov-Lipatov-Altarelli-Parisi (DGLAP) formalism [2, 3, 4, 5] of QCD to make predictions for deep inelastic scattering (DIS) cross-sections of leptons on hadrons. At low- x where the gluon density is rising rapidly it is probably necessary to go beyond the DGLAP formalism in order to sum $\ln(1/x)$ diagrams, as in the Balitsky-Fadin-Kuraev-Lipatov (BFKL) formalism [6, 7, 8] (for recent work see [9, 10, 11]). An alternative approach is to consider non-linear terms which describe gluon recombination as in the colour glass condensate model [12] which has had considerable success in explaining RHIC data [13]. A recent suggestion is to use a structure function consistent with HERA data that saturates the Froissart unitarity bound and thus predicts a $\ln^2 s$ dependence of the cross-section [14]. Such approaches are beyond the scope of the present paper, which is concerned with the more modest goal of estimating the uncertainties on high energy neutrino cross-sections which are compatible with the conventional NLO DGLAP formalism. The motivation is to provide an update on the neutrino cross-sections in the literature [15] which are widely used e.g. for estimating event rates in neutrino telescopes such as Baikal [16], ANTARES [17] and IceCube [18], cosmic ray observatories such as HiRes [19] and Auger [20], and radio detectors such as GLUE [21], FORTE [22], RICE [23] and ANITA [24]. As a corollary, if cross-sections much outside these limits are observed, it would be a clear signal of the need for extensions to conventional formalism. To date no unambiguous signals which require such extensions have been observed. The prospect for measuring the cross-section using very high energy cosmic neutrinos in order to distinguish between theoretical suggestions for gluon dynamics at low x has been discussed by us elsewhere [25].

Previous work on estimating high energy neutrino cross-sections [15] used PDF sets which no longer fit modern data from HERA [26] and an *ad hoc* procedure for estimating PDF uncertainties. The present work improves on this in several respects. Firstly, we use a recent PDF analysis which includes data from all HERA-I running [1]. Secondly, we take a consistent approach to PDF uncertainties — both model uncertainties and, more importantly, the uncertainties which derive from the correlated systematic errors of the input data sets [27]. Thirdly, we use NLO rather than LO calculations throughout. Fourthly, we use a general-mass variable flavour number scheme [28, 29] to treat heavy quark thresholds.

II. FORMALISM

Parton Density Function (PDF) determinations are global fits [1, 30, 32, 33, 34], which use inclusive cross-section data and structure function measurements from deep inelastic lepton hadron scattering (DIS) data. The kinematics of lepton hadron scattering is described in terms of the variables Q^2 , Bjorken x , and y which measures the energy transfer between the lepton and hadron systems.

The double differential charged current (CC) cross-section for neutrino and antineutrino production on isoscalar nucleon targets are given by [35],

$$\frac{d^2\sigma(\nu(\bar{\nu})N)}{dx dQ^2} = \frac{G_F^2 M_W^4}{2\pi(Q^2 + M_W^2)^2 x} \sigma_r(\nu(\bar{\nu})N) \quad (1)$$

where the reduced cross-sections $\sigma_r(\nu(\bar{\nu})N)$ are given by

$$\sigma_r(\nu N) = [Y_+ F_2^\nu(x, Q^2) - y^2 F_L^\nu(x, Q^2) + Y_- x F_3^\nu(x, Q^2)], \quad (2)$$

and

$$\sigma_r(\bar{\nu} N) = [Y_+ F_2^{\bar{\nu}}(x, Q^2) - y^2 F_L^{\bar{\nu}}(x, Q^2) - Y_- x F_3^{\bar{\nu}}(x, Q^2)], \quad (3)$$

where the structure functions F_2 , $x F_3$ and F_L are related directly to quark momentum distributions.

The QCD predictions for these structure functions are obtained by solving the DGLAP evolution equations at NLO in the $\overline{\text{MS}}$ scheme with the renormalisation and factorization scales both chosen to be Q^2 . These equations yield the PDFs at all values of Q^2 provided these distributions have been input as functions of x at some input scale Q_0^2 . The resulting PDFs are then convoluted with coefficient functions, in order to obtain the structure functions.

We use the PDF fit formalism of the published ZEUS-S global PDF analysis [1], but this fit is updated as follows. First, the range of the calculation has been extended up to $Q^2 = 10^{12}$ GeV² and down to $x = 10^{-12}$. Second, *all* inclusive cross-section data for neutral and charged current reactions from ZEUS HERA-I running (1994–2000) are included in the fit. Third, the parametrization is extended from 11 to 13 free parameters, input at $Q_0^2 = 7$ GeV². In summary, the PDFs for u valence quarks ($xu_v(x)$), d valence quarks ($xd_v(x)$), total sea quarks ($xS(x)$), and the gluon ($xg(x)$), are each parametrized by the form

$$p_1 x^{p_2} (1-x)^{p_3} P(x), \quad (4)$$

where $P(x) = 1 + p_5 x$. The strong coupling constant is taken to be $\alpha_s(M_Z^2) = 0.118$ [36]. The total sea contribution is $xS = 2x(\bar{u} + \bar{d} + \bar{s} + \bar{c} + \bar{b})$, where $\bar{q} = q_{\text{sea}}$ for each flavour, $u = u_v + u_{\text{sea}}$, $d = d_v + d_{\text{sea}}$ and $q = q_{\text{sea}}$ for all other flavours. The flavour structure of the light quark sea allows for the violation of the Gottfried sum rule such that $x(\bar{d} - \bar{u})$ is non-zero, but only the normalisation of this quantity is free, the shape being fixed in accordance with E866 Drell-Yan data [37]. A suppression of the strange sea with respect to the non-strange sea of a factor of 2 at Q_0^2 is also imposed, consistent with neutrino induced dimuon data from CCFR [38]. The normalisation parameters, p_1 , for the d and u valence and for the gluon are constrained to impose the number sum-rules and momentum sum-rule. The low- x shape parameters p_2 for the u and d valence quarks are set equal. Finally there are 13 free PDF parameters. Reasonable variations of these assumptions about the input parametrization are included in the model uncertainties on the output PDFs.

A more important source of uncertainties on the PDFs comes from the experimental uncertainties on the input data. The PDFs are presented with full accounting for uncertainties from correlated systematic errors (as well as from statistical and uncorrelated sources) using the conservative OFFSET method. The uncertainty bands should be regarded as 68% confidence limits. A full discussion of approaches to estimating PDF uncertainties is given in [1, 27]. The PDF uncertainties from this updated ZEUS-S-13 fit are comparable to those on the published ZEUS-S fit [1], as well as the most recent fits of the CTEQ [33, 34] and MRST [30, 32] groups.

Previous work [15] treated heavy quark production by using a zero-mass variable flavour number scheme, with slow-rescaling at the b to t threshold. Although, as explained in Section III, the exact treatment of the $b \rightarrow t$ threshold is not very important for the estimation of high energy neutrino cross-sections, it is important to use a correct treatment of heavy quark thresholds when determining the PDFs. We note that the central values of the sea quark distributions of the most recent CTEQ6.5 analysis [34] which uses a general mass variable flavour scheme for heavy quarks, lie *outside* the 90% CL uncertainty estimates of the previous CTEQ6.1 analysis [33], which used a zero-mass variable flavour number scheme (as did all previous CTEQ analyses). This difference is significant for lower Q^2 ($\lesssim 5000$ GeV²) and middling x ($5 \times 10^{-5} \lesssim x \lesssim 5 \times 10^{-2}$) and this is a kinematic region of relevance to the present study. The heavy quark production scheme used in the present fit is the general mass variable flavour number scheme of Roberts and Thorne [28, 29]. The central values of both the CTEQ6.5 PDF analysis [34] and the MRST2004 NLO analysis [31] (which also uses a general-mass variable flavour number scheme) lie within, or very close to, the uncertainty bands of the present analysis over the entire kinematic region of interest.

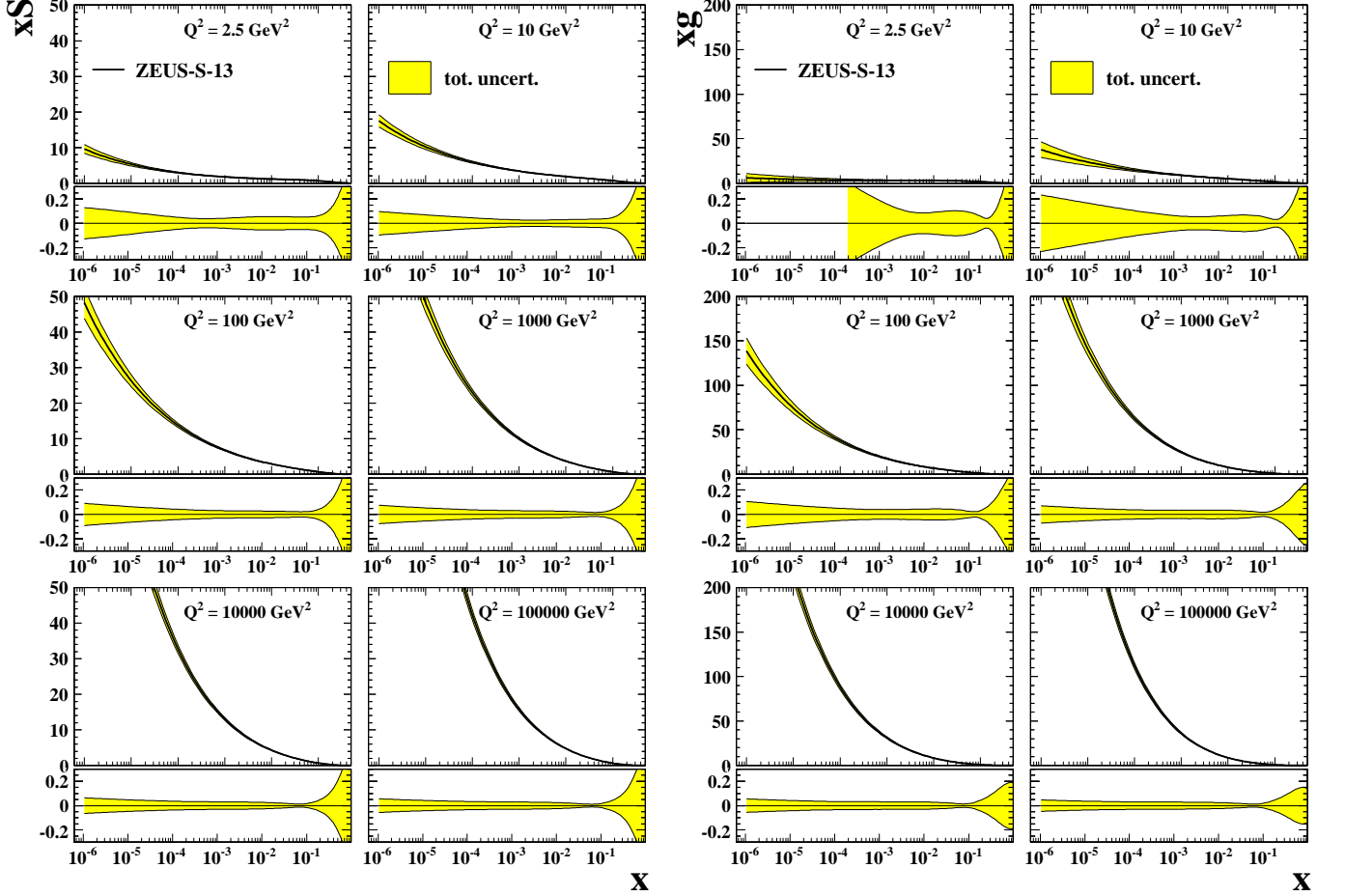


FIG. 1: The PDFs and their fractional uncertainties at various Q^2 are shown for sea quarks (left) and gluons (right).

III. RESULTS

At very small x and high Q^2 , the νN cross-section is dominated by sea quarks produced by gluon splitting $g \rightarrow q\bar{q}$. In this kinematic region, the parametrisation of the gluon momentum distribution is approximately: $xg(x, Q^2) \propto x^{-\lambda}$, where $\lambda \sim 0.3 - 0.4$. Figure 1 shows the predicted sea and gluon distributions from the present PDF fit and their fractional uncertainties, at various Q^2 values. This illustrates that the PDF uncertainties are largest at low Q^2 and at low- x . PDF uncertainties are also large at very high- x but this kinematic region is not important for scattering of high energy neutrinos.

In QCD at leading order, the longitudinal structure function F_L is identically zero, and the structure functions F_2 and xF_3 for neutrino interactions on isoscalar targets can be identified with quark distributions as follows:

$$F_2^\nu = x(u + d + 2s + 2b + \bar{u} + \bar{d} + 2\bar{c}), \quad xF_3^\nu = x(u + d + 2s + 2b - \bar{u} - \bar{d} - 2\bar{c}). \quad (5)$$

Similarly for antineutrino interactions,

$$F_2^{\bar{\nu}} = x(u + d + 2c + \bar{u} + \bar{d} + 2\bar{s} + 2\bar{b}), \quad xF_3^{\bar{\nu}} = x(u + d + 2c - \bar{u} - \bar{d} - 2\bar{s} - 2\bar{b}). \quad (6)$$

Assuming, $s = \bar{s}$, $c = \bar{c}$, $b = \bar{b}$, we obtain $F_2^\nu = F_2^{\bar{\nu}}$, whereas $xF_3^\nu - xF_3^{\bar{\nu}} = 2(s + \bar{s} + b + \bar{b} - c - \bar{c}) = 4(s + b - c)$. At NLO these expressions must be convoluted with appropriate coefficient functions (such that F_L is no longer zero) but these expressions still give us a good idea of the dominant contributions. Note however that the b contribution will be very suppressed until $Q^2 \gg M_t^2 \sim 3 \times 10^4 \text{ GeV}^2$, since the $b \rightarrow t$ coupling is dominant.

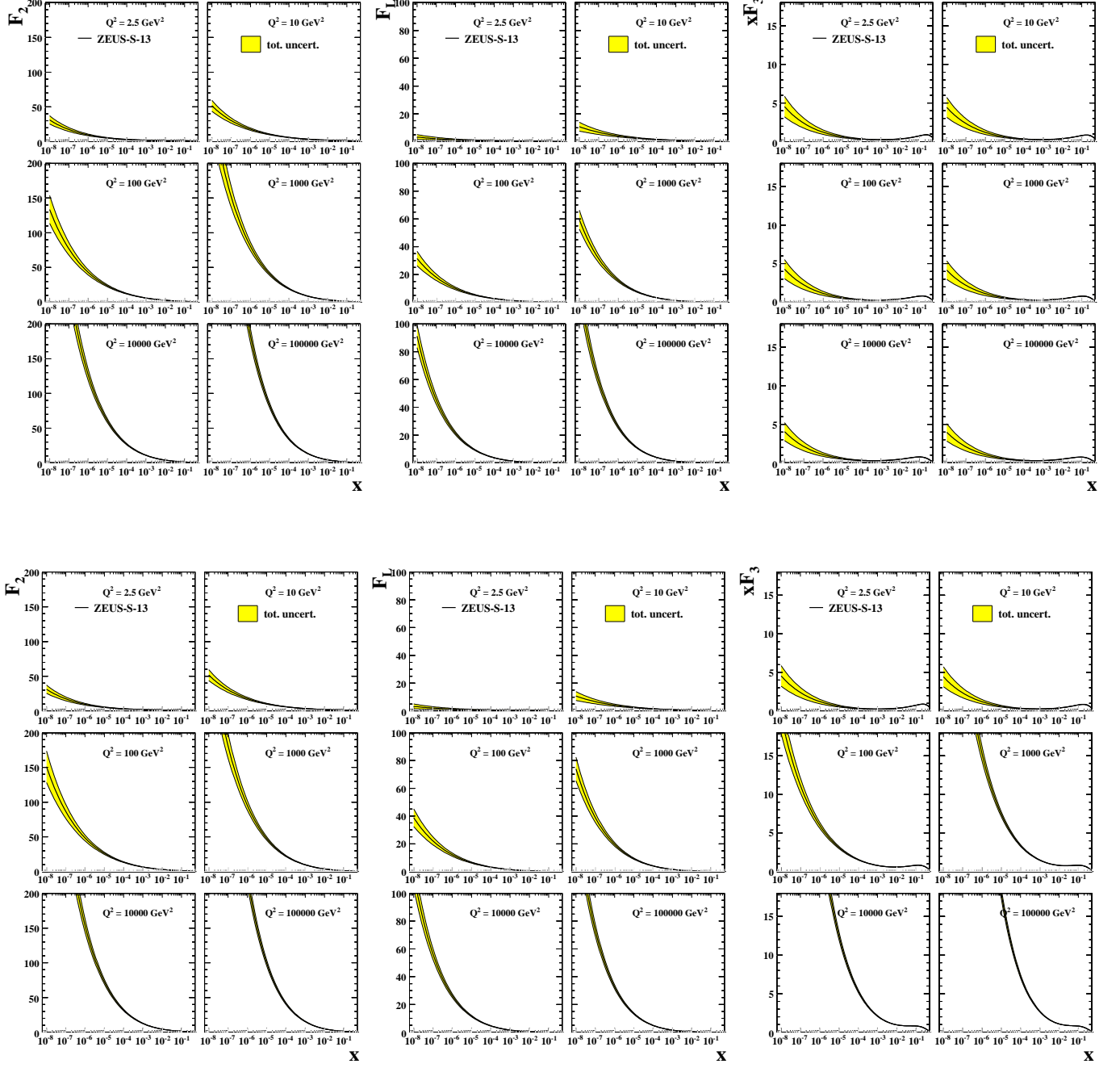


FIG. 2: Predictions for F_2^ν , F_L^ν and xF_3^ν using a zero mass variable flavour number scheme, without the b contribution (upper panels), and with the b contribution (lower panels).

In Figure 2 we show predictions for the neutrino structure functions F_2^ν , F_L^ν and xF_3^ν and in Figure 3 we show the antineutrino structure function $xF_3^{\bar{\nu}}$. In order to illustrate the potential impact of the b contribution, these were calculated using the coefficient functions of the zero-mass variable flavour number scheme with (lower panels) and without (upper panels) the b contribution. Note that the input PDFs were still determined using the general mass variable flavour number scheme.

The predictions for F_2 and F_L are somewhat suppressed without the b contribution, as is expected since the contribution of b to F_2 is at most 20%. However, the effect on xF_3 is much more dramatic. This can be understood

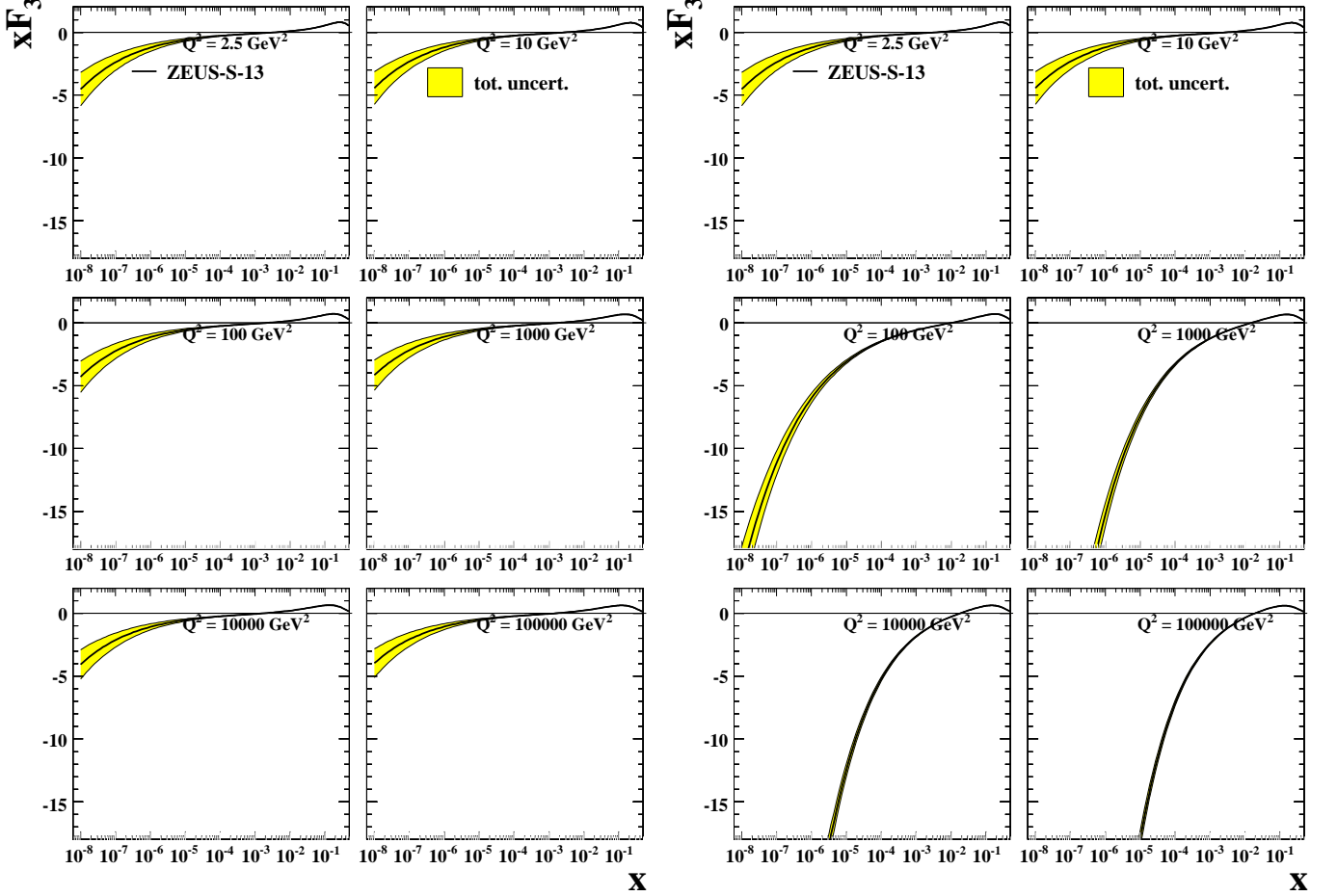


FIG. 3: Predictions for $xF_3^{\bar{\nu}}$ for antineutrinos using a zero mass variable flavour number scheme, without the b contribution (left panel), and with the b contribution (right panel).

by considering the LO expressions

$$xF_3^{\nu} = x(u_v + d_v + 2(s - \bar{c}) + 2b) \quad (7)$$

and

$$xF_3^{\bar{\nu}} = x(u_v + d_v + 2(c - \bar{s}) - 2\bar{b}). \quad (8)$$

At low- x the valence contributions are close to zero, while the strange and charm sea are of opposite sign and nearly equal, such that xF_3 is nearly all b quark and $xF_3^{\nu} \sim -xF_3^{\bar{\nu}}$.

Even though there are dramatic differences in predictions for xF_3 with and without the b contribution, this does not lead to significant differences in the νN and $\bar{\nu} N$ cross-sections because, at low- x , $xF_3 \lesssim F_2/5$, and the y dependence suppresses the contribution of xF_3 further. The b contribution to the reduced cross-section integrated over y is always less than $\sim 25\%$. However, in practice it is even more suppressed for CC processes since b is important only at higher $Q^2 (\gg M_t^2)$ because of the t threshold. Furthermore, in the total cross-section, the W propagator suppresses the contribution of the kinematic region $Q^2 \gg M_W^2$, such that contributions from $Q^2 \gg M_t^2$ are suppressed very significantly.

Figure 4 shows the predictions for the reduced neutrino cross-sections as a function of x for various Q^2 values above and below M_W^2 and M_t^2 . These illustrations have been made in terms of the reduced cross-section in order that one can see how the structure functions (hence the PDFs) contribute to the total cross-section. These cross-sections

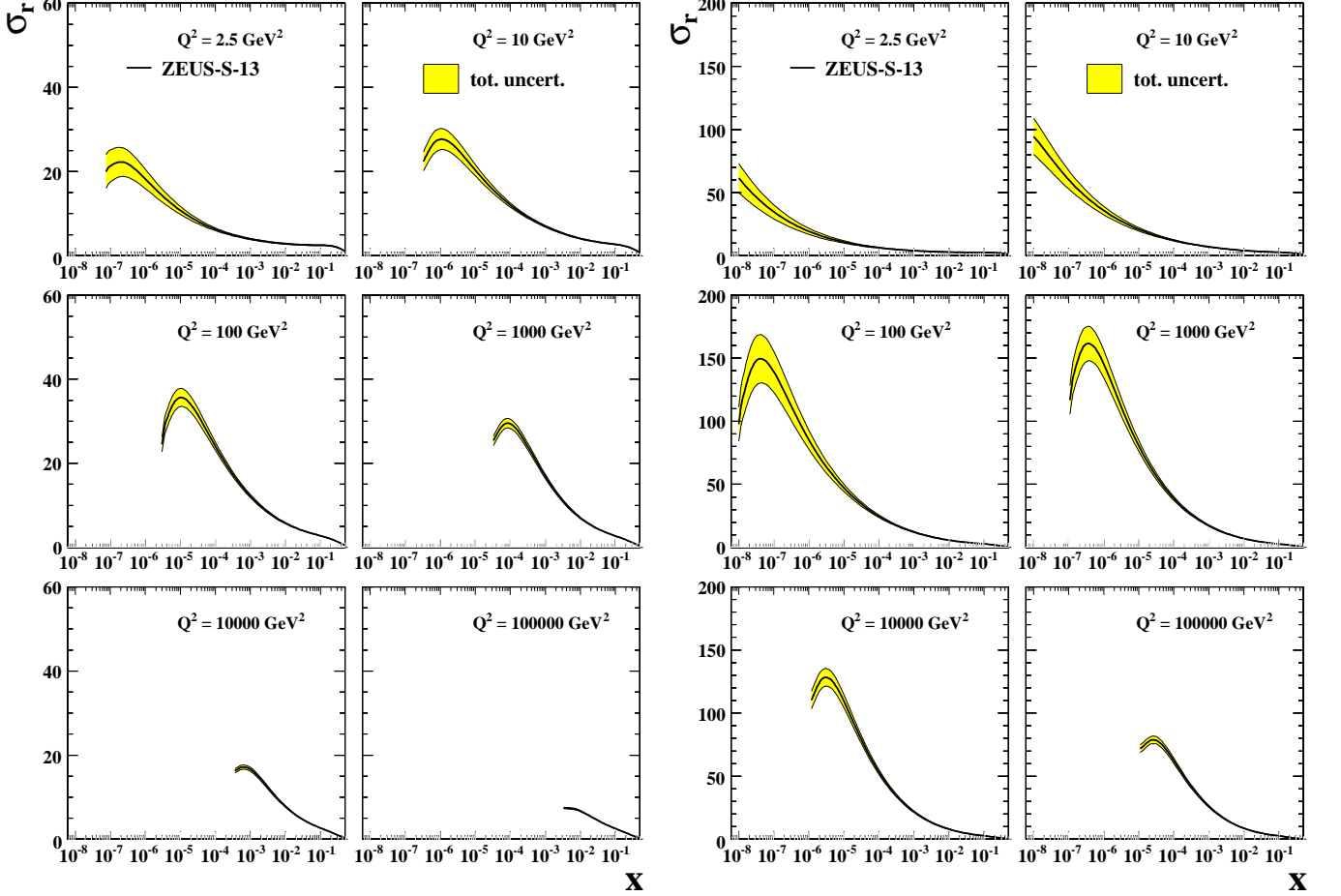


FIG. 4: Neutrino-nucleon reduced cross-sections for various Q^2 at $s = 3.6 \times 10^7 \text{ GeV}^2$ i.e. $E_\nu = 1.9 \times 10^7 \text{ GeV}$ (left panel), and $s = 10^{10} \text{ GeV}^2$ i.e. $E_\nu = 5.3 \times 10^9 \text{ GeV}$ (right panel).

have been calculated using the coefficient functions of the general-mass variable flavour scheme and are given for two representative values of the neutrino energy: $s = 3.6 \times 10^7 \text{ GeV}^2$ ($\Rightarrow E_\nu = 1.9 \times 10^7 \text{ GeV}$) and $s = 10^{10} \text{ GeV}^2$ ($\Rightarrow E_\nu = 5.3 \times 10^9 \text{ GeV}$). We do not show the antineutrino cross-sections separately because these are very close to the neutrino cross-sections at high energy. This is because the dominant structure function is $F_2^\nu = F_2^{\bar{\nu}}$, and although, $xF_3^\nu \sim -xF_3^{\bar{\nu}}$, the structure function xF_3 contributes with *opposite* sign in the neutrino and antineutrino cross-sections such that the net contribution of xF_3 is the same.

The restriction on the lowest value of x probed for each Q^2 value is explained by the effect of the kinematic cut-off, $y < 1$: since, $x = Q^2/sy$, we must have, $x > Q^2/s$. This kinematic cut-off ensures that higher Q^2 values do not probe very low- x until the neutrino energies are very high indeed. These figures illustrate which regions of x and Q^2 contribute most strongly to the reduced cross-section for the different neutrino energies. The dominant contributions come from $50 \lesssim Q^2 \lesssim 10^4 \text{ GeV}^2$ (where the exact region moves up gradually with s); the contribution of higher Q^2 ($Q^2 > M_W^2$) is suppressed by the W -propagator. For the lower energy $E_\nu = 1.9 \times 10^7 \text{ GeV}$, the important range is $10^{-6} \lesssim x \lesssim 10^{-3}$, while for the higher energy $E_\nu = 5.3 \times 10^9 \text{ GeV}$, this moves down to $10^{-8} \lesssim x \lesssim 10^{-4}$.

The PDF uncertainties are large at low- x and low Q^2 , but since the dominant contributions to the cross-section do *not* come from very low Q^2 values, the PDF uncertainty on the total neutrino cross-section is quite small even at the highest energies considered here: $s = 10^{12} \text{ GeV}^2$.

The total neutrino cross-sections are now obtained by integrating the predicted double differential cross-section

$d^2\sigma/dx dy$ with no cuts on either kinematic variable.¹ These cross-sections are tabulated in Table I at various values of s between 10^7 and 10^{12} GeV^2 , together with their uncertainties due to the PDFs, including both model uncertainties and the experimental uncertainties of the input data sets.² The trend of the PDF uncertainties can be understood by noting that as one moves to higher and higher neutrino energies one also moves to lower and lower x where the PDF uncertainties are increasing. These energies are relevant to e.g. the Auger experiment where cosmic neutrinos can be detected both as quasi-horizontal deeply penetrating air showers and (specifically ν_τ s) as Earth-skimming tau showers [20]. We have shown elsewhere [25] that the ratio of these two classes of events is a diagnostic of the νN cross-section, *independently* of the (rather uncertain) cosmic neutrino flux. The latter determines the absolute rates — e.g. assuming that extragalactic sources of the observed ultrahigh energy cosmic rays generate a neutrino flux saturating the “Waxman-Bahcall bound” [39], it would take 10 years of running with a $3 \times 10^4 \text{ km}^2$ array to tell whether the νN cross-section is suppressed significantly below the (unscreened) Standard Model prediction. Proposed satellite-borne detectors such as EUSO and OWL would scan even larger areas and achieve the necessary acceptance within a few years of running [40].

$s [\text{GeV}^2]$	$\sigma(\nu) [\text{pb}]$	PDF uncertainty
10^7	1252	$\pm 3\%$
2×10^7	1665	$\pm 3\%$
5×10^7	2391	$\pm 3.5\%$
10^8	3100	$\pm 4\%$
2×10^8	4022	$\pm 4.5\%$
5×10^8	5596	$\pm 5.5\%$
10^9	7135	$\pm 6\%$
2×10^9	9082	$\pm 6\%$
5×10^9	12333	$\pm 6.5\%$
10^{10}	15456	$\pm 7\%$
2×10^{10}	19379	$\pm 7\%$
5×10^{10}	25789	$\pm 8\%$
10^{11}	31865	$\pm 8\%$
2×10^{11}	39434	$\pm 9\%$
5×10^{11}	51635	$\pm 12\%$
10^{12}	63088	$\pm 14\%$

TABLE I: Neutrino-nucleon total CC cross-section, with the associated PDF uncertainty, at high energies.

Figure 5 compares our CC cross-section to the widely used leading-order calculation of Gandhi *et al* [15] which they fitted as: $(\sigma_{\text{CC}}^{\text{LO}}/\text{pb}) = 5.53(E_\nu/\text{GeV})^{0.363}$ for $10^7 \leq (E_\nu/\text{GeV}) \leq 10^{12}$. The present results show a less steep rise of the cross-section at high energies, reflecting the fact that more recent HERA cross-section data display a less dramatic rise at low- x than the early data which was used to calculate the CTEQ4-DIS PDFs. A power-law description is no longer appropriate over the whole range $10^7 \leq (E_\nu/\text{GeV}) \leq 10^{12}$, instead the relation

$$\ln\left(\frac{\sigma_{\text{CC}}^{\text{NLO}}}{\text{pb}}\right) = \ln(10^{36}) - 98.8 \left[\ln\left(\frac{E_\nu}{\text{GeV}}\right) \right]^{-0.0964}, \quad (9)$$

fits the calculated cross-section to within $\sim 10\%$ (P. Mertsch, private communication).

Neutrino telescopes such as IceCube are optimised to probe lower energies of order a TeV [18]. In this case the high- x region becomes important and the neutrino and antineutrino cross-sections are *different* because the valence contribution to $x F_3$ is now significant. In Table II we give both neutrino and antineutrino cross-sections for values of s between 10^2 and 10^7 GeV^2 , together with estimates of their PDF uncertainties. The onset of the linear dependence of the cross-section on s for $s < M_W^2$ can be seen and in Figure 6 we compare the calculated σ/E_ν with some available recent experimental measurements [41, 42], from the compendium on the Durham-HEPDATABASE database [43]. The

¹ Experiments may have specific cuts on e.g. y and we are happy to provide the differential cross-section for use in simulation programmes.

² Note that these are somewhat smaller than as shown in our previous work [25] since we have now carefully evaluated the effect of heavy quark thresholds on the DGLAP evolution, which had been added on previously as a systematic uncertainty.

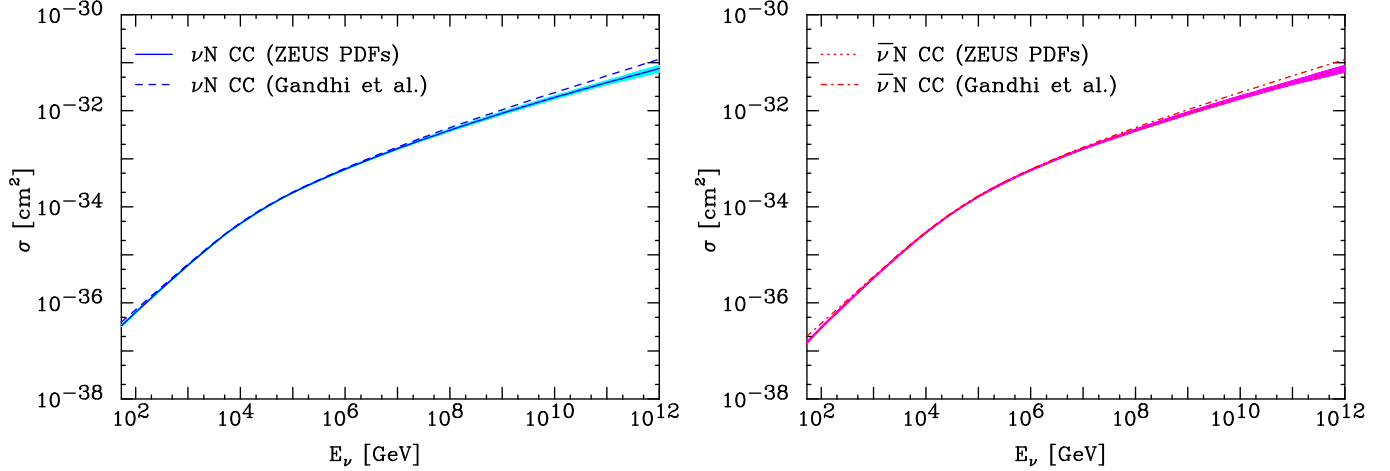


FIG. 5: The total CC cross-section at ultra high energies for neutrinos (left) and antineutrinos (right) along with the $\pm 1\sigma$ uncertainties (shaded band), compared with the previous calculation by Gandhi *et al* [15].

agreement is quite good, given in particular that our predictions are made for $Q^2 > 1 \text{ GeV}^2$ (since perturbative QCD cannot be used at lower values); for $s \lesssim 100 \text{ GeV}^2$, there can be contributions of $\mathcal{O}(10\%)$ from even lower values of Q^2 which are *not* accounted for here. However there are also corrections for nuclear shadowing which ought to suppress the cross-section by a comparable amount. A recent discussion of such effects can be found in ref.[44].

The trend of the PDF uncertainties can be understood as follows: as one moves to lower neutrino energies one moves out of the very low- x region such that PDF uncertainties decrease. These uncertainties are smallest at $10^{-2} \lesssim x \lesssim 10^{-1}$, corresponding to $s \sim 10^5$. Moving to yet lower neutrino energies brings us into the high- x region where PDF uncertainties are larger again.

$s [\text{GeV}^2]$	$\sigma(\nu) [\text{pb}]$	PDF uncertainty	$\sigma(\bar{\nu}) [\text{pb}]$	PDF uncertainty
10^2	0.334	$\pm 3\%$	0.151	$\pm 4\%$
2×10^2	0.676	$\pm 2.5\%$	0.327	$\pm 3.5\%$
5×10^2	1.69	$\pm 2.5\%$	0.864	$\pm 3.5\%$
10^3	3.32	$\pm 2\%$	1.76	$\pm 3\%$
2×10^3	6.47	$\pm 2\%$	3.55	$\pm 2.5\%$
5×10^3	15.0	$\pm 2\%$	8.67	$\pm 2.5\%$
10^4	27.6	$\pm 2\%$	16.6	$\pm 2.5\%$
2×10^4	47.0	$\pm 2\%$	30.8	$\pm 2\%$
5×10^4	89.4	$\pm 2\%$	64.8	$\pm 2\%$
10^5	138	$\pm 1.5\%$	107	$\pm 1.5\%$
2×10^5	204	$\pm 2\%$	171	$\pm 2\%$
5×10^5	326	$\pm 2\%$	293	$\pm 2\%$
10^6	454	$\pm 2\%$	423	$\pm 2\%$
2×10^6	628	$\pm 2.5\%$	600	$\pm 2.5\%$
5×10^6	937	$\pm 2.5\%$	915	$\pm 2.5\%$

TABLE II: Total CC cross-section for neutrinos and antineutrinos with their associated uncertainties at medium energies.

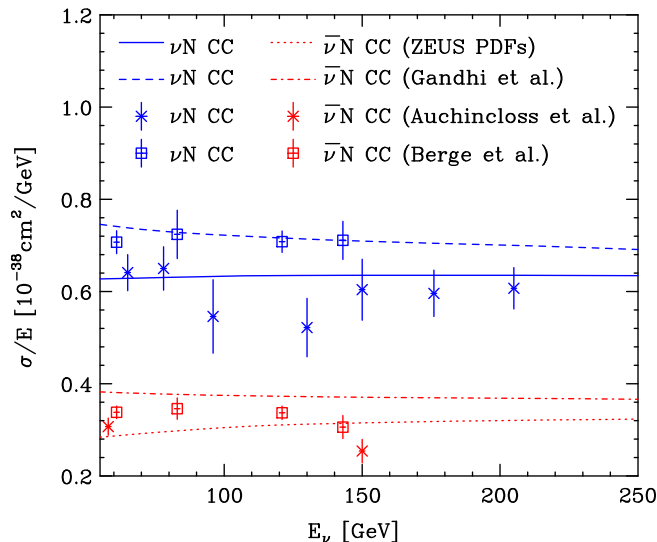


FIG. 6: The total CC cross-sections at medium energies for neutrinos and antineutrinos compared with the previous calculation by Gandhi *et al* [15] and with selected experimental data.

IV. CONCLUSIONS

We have calculated the charged current neutrino cross-section at NLO in the Standard Model using the best available DIS data along with a careful estimate of the associated uncertainties. As mentioned earlier, there are further uncertainties associated with QCD effects at very low x which are not addressed in the DGLAP formalism. When x is sufficiently small that $\alpha_s \ln(1/x) \sim 1$, it is necessary to resum these large logarithms using the BFKL formalism. Whereas such calculations at leading-log suggest an even steeper rise of the gluon structure function at low x (which would imply a higher $\nu - N$ cross-section), this rise is not so dramatic at next-to-leading-log; for a recent application of NLL BFKL resummation to deep inelastic scattering see [45]. Moreover both the DGLAP and the BFKL formalisms neglect non-linear screening effects due to gluon recombination which may lead to saturation of the gluon structure function. This has been modelled in the colour dipole framework in which DIS at low x is viewed as the interaction of the $q\bar{q}$ dipole to which the gauge bosons fluctuate. An unified BFKL/DGLAP calculation [46] supplemented by estimates of screening and nuclear shadowing effects, predicts a *decrease* of the $\nu - N$ cross-section by 20 – 100% at very high energies $E_\nu \sim 10^8 - 10^{12}$ GeV [47]. An alternative approach uses the colour glass condensate formalism [12] and predicts a similar suppression when a dipole model [48] which fits data from RHIC is used [49]. The predicted cross-section is even lower [49] if a different dipole model [50] developed to fit the HERA data is used and the gluon distribution is assumed to decrease for $x < 10^{-5}$. Other possibilities for the behaviour of the high energy $\nu - N$ cross-section have also been discussed [14, 51].

Detectors for UHE cosmic neutrinos would be able to probe such new physics if they can establish deviations from the perturbative DGLAP prediction. Hence we recommend our calculated values for estimation of the baseline event rates in neutrino telescopes and for use in event generators such as ANIS [52]. While the expected neutrino fluxes (e.g. from the sources of the observed high energy cosmic rays) are rather uncertain, experiments can in principle exploit the different dependence on the cross-section of the rate of Earth-skimming and quasi-horizontal events [25].

Acknowledgments

We thank Robert Thorne for discussions and Claire Gwenlan and Philipp Mertsch for help with the figures. SS acknowledges a PPARC Senior Fellowship (PPA/C506205/1) and the EU network “UniverseNet” (MRTN-CT-2006-035863); he wishes to thank colleagues in Auger and IceCube for encouragement to publish this study.

[1] S. Chekanov *et al.* [ZEUS Collaboration], Phys. Rev. D **67** (2003) 012007.

- [2] G. Altarelli and G. Parisi, Nucl. Phys. B **126** (1977) 298.
- [3] V. N. Gribov and L. N. Lipatov, Sov. J. Nucl. Phys. **15** (1972) 438.
- [4] L. N. Lipatov, Sov. J. Nucl. Phys. **20** (1975) 94.
- [5] Y. L. Dokshitzer, Sov. Phys. JETP **46** (1977) 641.
- [6] E. A. Kuraev, L. N. Lipatov and V. S. Fadin, Sov. Phys. JETP **45** (1977) 199.
- [7] I. I. Balitsky and L. N. Lipatov, Sov. J. Nucl. Phys. **28** (1978) 822.
- [8] L. N. Lipatov, Sov. Phys. JETP **63** (1986) 904.
- [9] C. D. White and R. S. Thorne, Phys. Rev. D **74** (2006) 014002.
- [10] G. Altarelli, R. D. Ball and S. Forte, Nucl. Phys. B **742** (2006) 1.
- [11] M. Ciafaloni, D. Colferai, G. P. Salam and A. M. Stasto, Phys. Lett. B **635** (2006) 320.
- [12] E. Iancu and R. Venugopalan, in *Quark Gluon Plasma*, eds. R.C. Hwa and X.-N. Wang, World Scientific [arXiv:hep-ph/0303204].
- [13] J. Jalilian-Marian and Y. V. Kovchegov, Prog. Part. Nucl. Phys. **56** (2006) 104.
- [14] E. L. Berger, M. M. Block, D. W. McKay and C. I. Tan, arXiv:0708.1960 [hep-ph].
- [15] R. Gandhi, C. Quigg, M. H. Reno and I. Sarcevic, Phys. Rev. D **58** (1998) 093009.
- [16] K. Antipin *et al.*, Nucl. Phys. Proc. Suppl. **168** (2007) 296.
- [17] E. Aslanides *et al.* [ANTARES Collaboration], arXiv:astro-ph/9907432.
- [18] A. Achterberg *et al.* [IceCube Collaboration], Phys. Rev. D **75** (2007) 102001; Phys. Rev. D **76** (2007) 027101; Phys. Rev. D **76** (2007) 042008; Astrophys. J. **664** (2007) 397; arXiv:0711.3022 [astro-ph].
- [19] K. Martens [HiRes Collaboration], arXiv:0707.4417 [astro-ph].
- [20] J. Alvarez-Muniz [Pierre Auger Collaboration], Proc. 30th International Cosmic Ray Conference, Merida (2007); O. B. Bigas [Pierre Auger Collaboration], arXiv:0712.1909 [astro-ph].
- [21] P. W. Gorham, C. L. Hebert, K. M. Liewer, C. J. Naudet, D. Saltzberg and D. Williams, Phys. Rev. Lett. **93** (2004) 041101.
- [22] N. G. Lehtinen, P. W. Gorham, A. R. Jacobson and R. A. Roussel-Dupre, Phys. Rev. D **9** (2004) 013008.
- [23] I. Kravchenko *et al.* [RICE Collaboration], Astropart. Phys. **20** (2003) 195.
- [24] S. W. Barwick *et al.* [ANITA Collaboration], Phys. Rev. Lett. **96** (2006) 171101.
- [25] L. A. Anchordoqui, A. M. Cooper-Sarkar, D. Hooper and S. Sarkar, Phys. Rev. D **74** (2006) 043008.
- [26] W. K. Tung, Proc. DIS 2004, eds. D. Bruncko *et al.* [arXiv:hep-ph/0409145].
- [27] A. M. Cooper-Sarkar, J. Phys. G **28** (2002) 2669.
- [28] R. S. Thorne and R. G. Roberts, Phys. Rev. D **57** (1998) 6871.
- [29] R. S. Thorne, Phys. Rev. D **73** (2006) 054019.
- [30] A. D. Martin, R. G. Roberts, W. J. Stirling and R. S. Thorne, Eur. Phys. J. C **23** (2002) 73.
- [31] A. D. Martin, R. G. Roberts, W. J. Stirling and R. S. Thorne, Phys. Lett. B **604** (2004) 61.
- [32] A. D. Martin, W. J. Stirling, R. S. Thorne and G. Watt, Phys. Lett. B **652** (2007) 292.
- [33] J. Pumplin, D. R. Stump, J. Huston, H. L. Lai, P. Nadolsky and W. K. Tung, JHEP **0207** (2002) 012.
- [34] W. K. Tung, H. L. Lai, A. Belyaev, J. Pumplin, D. Stump and C. P. Yuan, JHEP **0702** (2007) 053.
- [35] R. Devenish and A. Cooper-Sarkar, *Deep Inelastic Scattering*, Oxford University Press (2004).
- [36] S. Eidelman *et al.* [Particle Data Group], Phys. Lett. B **592** (2004) 1.
- [37] E. A. Hawker *et al.* [FNAL E866/NuSea Collaboration], Phys. Rev. Lett. **80** (1998) 3715.
- [38] A. O. Bazarko *et al.* [CCFR Collaboration], Z. Phys. C **65** (1995) 189.
- [39] E. Waxman and J. N. Bahcall, Phys. Rev. D **59** (1999) 023002.
- [40] S. Palomares-Ruiz, A. Irimia and T. J. Weiler, Phys. Rev. D **73** (2006) 083003.
- [41] P. S. Auchincloss *et al.*, Z. Phys. C **48** (1990) 411.
- [42] J. P. Berge *et al.*, Z. Phys. C **35** (1987) 443.
- [43] M. R. Whalley, Nucl. Phys. Proc. Suppl. **139** (2005) 241.
- [44] N. Armesto, C. Merino, G. Parente and E. Zas, arXiv:0709.4461 [hep-ph].
- [45] C. D. White and R. S. Thorne, Phys. Rev. D **75** (2007) 034005.
- [46] J. Kwiecinski, A. D. Martin and A. M. Stasto, Phys. Rev. D **59** (1999) 093002.
- [47] K. Kutak and J. Kwiecinski, Eur. Phys. J. C **29** (2003) 521.
- [48] D. Kharzeev, Y. V. Kovchegov and K. Tuchin, Phys. Lett. B **599** (2004) 23.
- [49] E. M. Henley and J. Jalilian-Marian, Phys. Rev. D **73** (2006) 094004.
- [50] J. Bartels, K. Golec-Biernat and H. Kowalski, Phys. Rev. D **66** (2002) 014001.
- [51] J. Jalilian-Marian, Phys. Rev. D **68** (2003) 054005 [Erratum-ibid. D **70** (2004) 079903]; M. V. T. Machado, Phys. Rev. D **70** (2004) 053008; R. Fiore, L. L. Jenkovszky, A. V. Kotikov, F. Paccanoni, A. Papa and E. Predazzi, Phys. Rev. D **71** (2005) 033002; R. Fiore, L. L. Jenkovszky, A. V. Kotikov, F. Paccanoni and A. Papa, Phys. Rev. D **73** (2006) 053012.
- [52] A. Gazizov and M. P. Kowalski, Comput. Phys. Commun. **172** (2005) 203.